Investigation of Materials for Long Life, High Reliability Flexure Bearing Springs for Stirling Cryocooler Applications

C.J. Simcock

Honeywell Hymatic
University of Birmingham
England

ABSTRACT

Flexure bearing disc springs are installed to support the compressor motor assembly and the displacer within the linear Stirling cryocooler. Such Spring components are photo-etched in stainless steel. As the spring fatigue failure is critical; time consuming batch tests are performed. Research has been carried out to identify an acceptable factor of safety for the component, establish material mechanical properties and improve the understanding of failure and its causes. Operating within a safe limit and inspecting for intolerable defects removes the need for extended batch testing.

Finite Element Analysis (FEA) modeling has been used to understand spring stress versus displacement stroke. To validate FEA model results, strain gauges were fitted to the components subjected to the representative loading. A good correlation of the results supports the use of FEA modelling for design optimization of flexure bearing springs. Assemblies using the components optimized for the maximum stroke require superior quality control and batch testing. Other designs, operating more comfortably within their performance envelope, may proceed through build without rigorous quality and batch tests.

INTRODUCTION

Flexure Bearing Springs

In an effort to improve lifetime and reliability of coolers, specifically for space applications, advances have been made in both compressor and cold head designs. Dr. Gordon Davey of the University of Oxford pioneered work on long-life compressors in the early 1980s.[1] Compressor development concentrated on the removal of rubbing contact between the piston and cylinder. Lubricants would contaminate the system and dry-bearings would necessitate wear. In these oil-free compressors, wear of rubbing seals limits compressor lifetime. By suspending the cylinder, it moves concentrically without touching the piston. Flexure bearings that support the piston and the displacer inside their respective cylinders eliminate the rubbing contacts. Such flexure bearing springs are found in the Honeywell Hymatic Stirling cooler designs, the development of which was published, based on Oxford technology.[2] In common with all of the Honeywell Hymatic Stirling cooler products, the design utilizes flexure bearings to suspend the compressors and cold head

displacer ensuring that the clearance seals are preserved under all operational conditions, hence eliminating component wear and creation of debris as a failure mechanisms.

Clearance is critical to minimize gas leakage. By very accurate machining, the gap between the piston and the cylinder can be reduced to microns. This clearance gap impedes the flow and acts as a dynamic seal for the helium gas in the system. Friction (static and dynamic) and alignment tests in the assembly process ensure frictionless movement. The importance of linear movement is well reported.[3]

The flexure bearings inside the compressor are critical to guaranteed long lifetimes. Honeywell Hymatic Stirling cryocoolers have demonstrated a five year maintenance free continuous operation, and product life is expected to exceed ten years. The flexure bearing springs ensure that the piston is fully supported and only allowed translation in an axial direction. The design principle of a flexure bearing allows for large movement in the axial direction, i.e. is less stiff in the axial direction, yet possesses a very high stiffness in radial direction to maintain component clearances.

The stress analysis of a component such as a flexure bearing spring is quite complex. The component is likely to experience large deformations as a result of simultaneous shear, torsion and bending of varying-width 'arms'. The flexure-bearing spring designs may be optimized through the use of FEA. By modeling the springs, it is possible to identify the location of maximum stresses and optimize the radial stiffness. FEA modeling of a flexure bearing disc with three spiral slots identified the dependence of maximum stresses on the spiral profile, diameter and thickness of the component.[4] This research outlined three design requirements; fatigue strength, radial stiffness and axial stiffness.

Associated Research (Carried out by CJ Simcock during the Course of EngD Study)

In the testing of thin-sheet photo-etched material; multiple grades of stainless steel have been investigated. A superior grade demonstrated improved fatigue properties over the current composition; offering the opportunity of an increased spring stroke and improved cooler efficiencies. The multiple spring 'stack' arrangement varied with both movement and stresses experienced by a single component. The etching process was found not to compromise surface finish integrity. However, pits (a likely result of etch defect) in the test samples have been identified as initiation points for failure.

OBJECTIVES

The experimental aims are as follows:

· To improve understanding of spring displacement stroke versus stress.
· To identify characteristics of spring stress regions.
· To correlate FEA model predictions with strain gauge measurements with a view to validation of modelling as a design optimization tool.
· To develop evidence which would permit reduced batch testing of mainstream, high-throughput commercial Stirling cryocooler springs.

EXPERIMENTAL METHOD

For the purposes of all testing, three locations of interest were identified; A, B, and C, (see Fig. 1). Locations A and B were considered to be uniform stress regions which would offer good opportunities for accommodating strain gauge footprint. Location C was identified as a high stress region. When the spring arm is modeled as a simple beam subjected to bending, the thinnest section falls at the centre of the length, the point of maximum stress.

As experience had indicated variances in both the movement and the stress experienced, stack effects were also considered. FEA was carried out on both the single and multi-spring stacks. Stresses were compared (in preference to strains) in keeping with the preceding associated research which established the tensile and fatigue properties of the spring material. Stresses are also somewhat easier to 'visualize'.
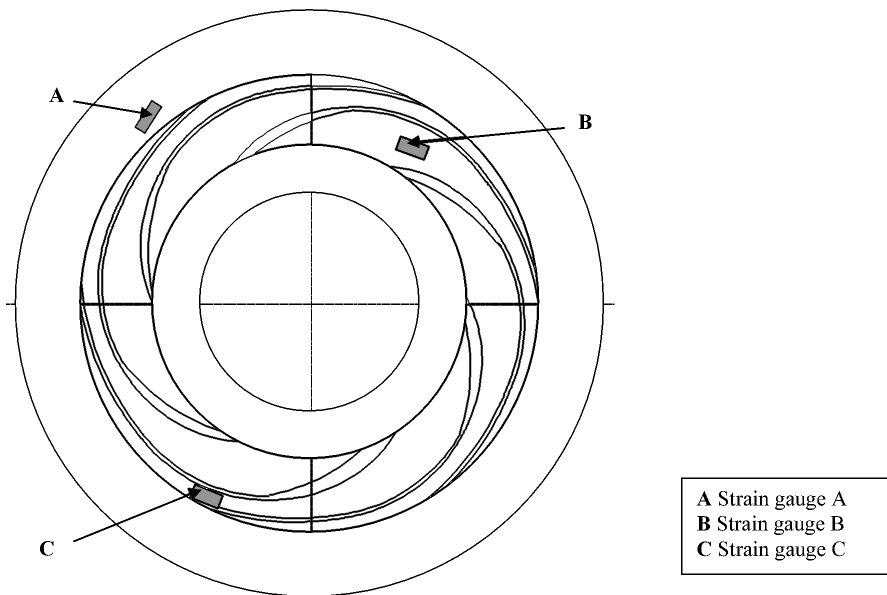
Figure 1. Location of strain gauges, A, B and C on a notional representative Spring.

Finite Element Analysis

ANSYS Workbench (Multiphysics Version, Release 10.0) was selected as the modeling software. Nonlinear techniques were used with advanced global control, an aggressive shape-checker and low solid element order. Command driven code was employed to optimize the mesh for thin sheet components.

The single spring model was composed of 38,846 quadrilateral elements, of 0.25 mm in size. Repetitions of the solutions utilizing a 0.5 mm element indicated results within 1 MPa in locations A and B, and within 4 MPa at location C. The double spring stack model was constructed of four bodies, including 31,813 quadrilateral elements of 0.5 mm in size (Physical memory restrictions prevented the solving of this model using 0.25 mm elements). In this multi-spring arrangement, the geometry of the thin-sheet springs were separated by 10 mm Inner and Outer components. Solutions of both the displacement (in mm) and the equivalent (von-Mises) stress (in MPa) were calculated.

Strain Gauge

Twelve 1 mm Kyowa strain gauges (KFG-1N-120-C1-11) were fitted to four spring components using cyanoacrylate base cement (CC-33A). The springs were assembled in a product representative stack. Fully insulated 0.089 mm nominal diameter enamel coated copper wire (J-W-1177/15) was soldered to the gauge wires to enable interface with a quarter-bridge Wheatstone bridge circuit. Displacement was controlled manually, driving the hydraulics to an accuracy of 0.01 mm. Measurements were taken at 1 mm intervals up to an 11.56 mm maximum test stroke. The spring stack was displaced using a purpose-built fixture secured to an ESH™ two column servo hydraulic testing machine.

For linear-elastic materials such as steel, Hooke's Law (eq. 1) is valid throughout the elastic range (i.e. below the yield strength):

$$\sigma = E.\varepsilon \qquad (1)$$

Measured resultant strains (ε) were transposed to stresses (σ) applying Young modulus (E). Note: All stresses measured during the course of this experimentation were within the elastic limit

of the base material. Additional research conducted has confirmed that the material has a linear stress-strain relation and a yield strength in excess of 950 MPa.

Spring Cycling

A product representative stack of springs was driven to a control stroke (see Fig. 2) to confirm that the FEA model correctly identified the region of maximum stress at full deflection. The cycling was conducted on common equipment with the strain gauge testing, using a purpose-built fixture secured to an ESH™ two column servo hydraulic testing machine. Due to the limitations of the hydraulic testing machine, the springs were subjected to half-cycles only, i.e. spring displacement was +11.56 mm, not ±11.56 mm about the mean at rest position. A sine wave input was used to excite the spring at a rate of 1 Hz, and cycles were monitored by an electronic counter.

EXPERIMENTAL RESULTS AND DISCUSSION

FEA and Strain Gauge

FEA modeling suggested a maximum stress of 744 MPa at the maximum spring stroke. This maximum can be found at the corner of the inner edge of the thin section of the spiral. At low stroke displacements, (below 7 mm) the FEA model indicates that bands of high stress exist across the inner edge of the spiral. The maximum stress at such low strokes is located at the inner edge of the spiral, near the end of the cutout. At strokes of 7 mm and above, the maximum stress indicated was consistently at the inner edge of the thin section, at the midpoint of the spiral arm. At higher strokes, the regions of the maximum stress became more localized.

Gauge Location A. Comparison of FEA and strain gauge results revealed strong correlation (see Fig. 3). Ninety one percent (91%) of all the strain gauge results were within 35 MPa of the single spring FEA model predicted stress. Comparing the FEA models, the double spring stresses at location A were within 6 MPa of the single spring results, and the upper and lower spring results were within 1 MPa of each other.
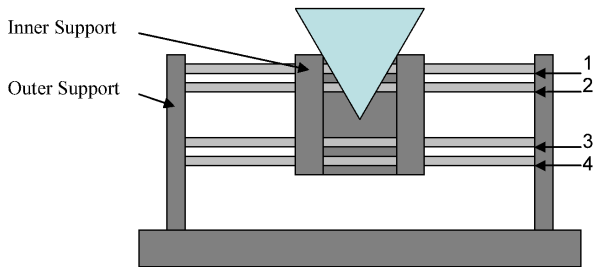

Figure 2. Schematic of the spring stack, numbers indicating springs 1 to 4.
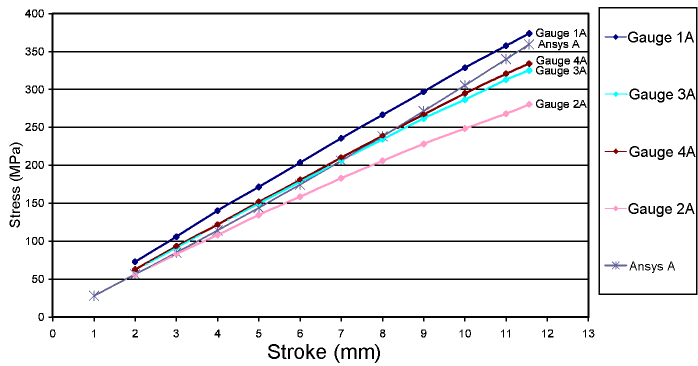

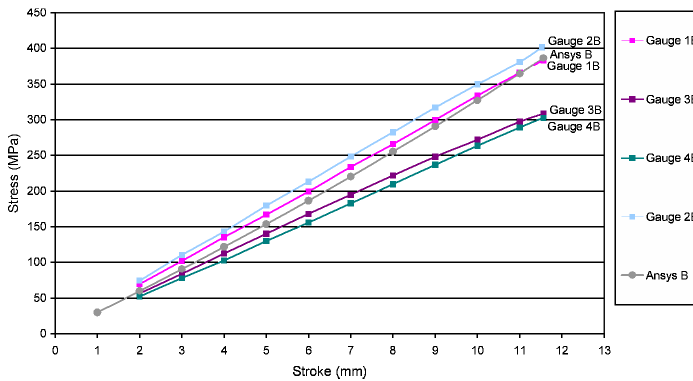**Figure 3.** Stroke versus stress, location A.

Figure 4. Stroke versus stress, location B.

Gauge Location B. Correlation between the FEA and strain gauge data was also very good (see Fig. 4). All of the results for springs 1 and 2 were within 28 MPa of the FEA predicted stress. Over 77% of strain gauge data were within 35 MPa of the single spring FEA model predicted stress. Only at an increased stroke did the data vary. The maximum deviation between the FEA and the strain gauge indicated stresses was 83 MPa at a maximum stroke for spring 4. Comparing the FEA models, the double spring stresses at location B were within 4 MPa of the single spring results, and the upper and lower spring results were within 1 MPa of each other.

Gauge Location C. Over 75% of the strain gauge data was within 50 MPa of the single spring FEA model predicted stress at location C. The maximum deviation between the FEA and the strain gauge indicated stresses was 61 MPa at 6 mm stroke, for spring 4. The difficulties associated with the positioning of the gauges at location C were evident throughout the experiment. The width of the component section makes the placement of a gauge difficult, and the nature of the forces involved made the strain measurement challenging. The strain gauge data indicated mixed results; suggesting the sensitivity of monitoring in this region. Of the four gauges located in this area, one gauge became delaminated the gauge on the third spring, i.e. 3C. As a consequence, data from this gauge has not been included. In the strain measurement, tests were repeated on the rising and the falling stroke to validate results. After the test, the fixture was reversed and the process repeated to establish if the results were affected by the material-gauge thickness. Multiple tests confirmed the repeatability of the testing, and the thickness effects were eliminated.

The FEA model also struggled with the calculation of information at probe location C. At locations A and B, stresses logically increased with a corresponding stroke. The FEA solution probe positioned at location C indicated a leveling off of stress in relation to stroke, and a reduction in stress at strokes in excess of 10 mm (see Fig. 5). Further, though the results for the single spring
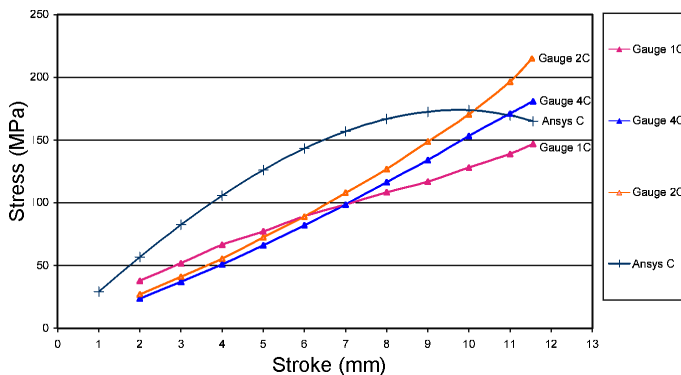

Figure 5. Stroke versus stress, location C. Note the non-linearity of the ANSYS prediction.
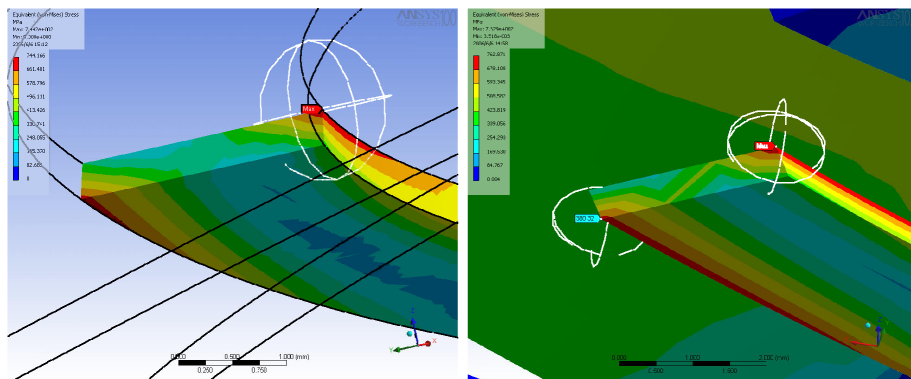
Figure 6. Cross-section of single and double Spring model at maximum test stroke at mid-point of Spring arm. Maximum stresses of 744 MPa and 763 MPa respectively.

versus the double spring FEA model in locations A and B were very consistent. This was not the case at location C. The probe positioned at location C indicated that stresses for both of the springs in the stack were twice those calculated for the single spring model. Probing of the solution identified that this was simply a result of the massive stress gradient across the component cross-section at this point. The two models indicate very similar results; similar maximum values and near-identical stress distributions (see Fig. 6). Small variations may be attributed to the differences in mesh. At this point, it is mindful to note that the strain gauge acts in one direction, capturing only an average of the stresses experienced, whereas the FEA model can be used to identify multidirectional stresses, and in this case indicates the criticality of position in relation to stress.

Summary and Additional Discussion. Considering all strain gauge data collected, over 85% was within 50 MPa of the single spring FEA model, and 71% was within 35 MPa of FEA predictions. All data was found to be comfortably within 100 MPa of FEA model predictions.

The FEA model assumes that the spring has parallel sides. Due to the nature of the double-sided photo-etching process, the manufactured component is not square in section; it exhibits a 'cusp' (reference SEM image of fracture face, Fig. 9). This may be considered to be a stress raiser; however, SEM analysis of the fracture faces of the springs exposed to high-cycle fatigue has not suggested that this feature has a detrimental effect on the component life.

Spring Cycling

The spring stack survived over a million cycles at the maximum test stroke (11.56 mm) without a failure. To force a failure, with a maximum cycling capability of 1 Hz, the stroke was increased to 16 mm. The servo hydraulic testing machine was set up to trip upon detecting under-loading. After 34,400 machine cycles at 150% test stroke, it tripped to shutdown the hydraulics. All four springs were found to have suffered breakage in one or more places. All breakages were located at the midpoints of the spring arm, where cross-sectional area is a minimum.

Spring 3 failed in three positions (see Fig. 7). Spring 4 suffered one breakage and another crack had formed beyond the midpoint of the section (see Fig. 8). This finding confirms that the crack initiated from the inner surface of the spring arm. Springs 1 and 2 also suffered one breakage each. No additional partial fractures were evident.

Examination of the fracture faces by an SEM revealed further evidence relating to the mode of failure; spring 1 is featured as an example. In Fig. 9, the crack initiated at the base of the image (i.e. the inner edge at the centre of the spring arm). Striations indicate the direction of crack travel. Signs of fast fracture are visible towards the top of the face, (1), and the very top 'layered' section suggests overload and final failure (2).
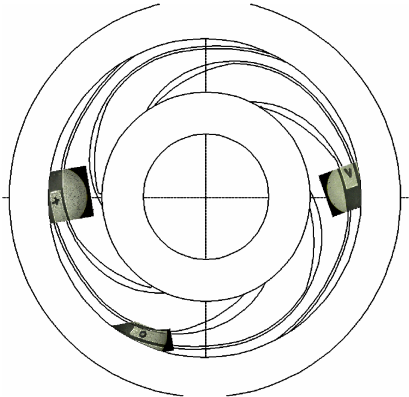
Figure 7. Spring 3 fracture location photography on notional representative Spring schematic. Note that the remaining Spring arm pieces have been removed for clarity in the photographs.
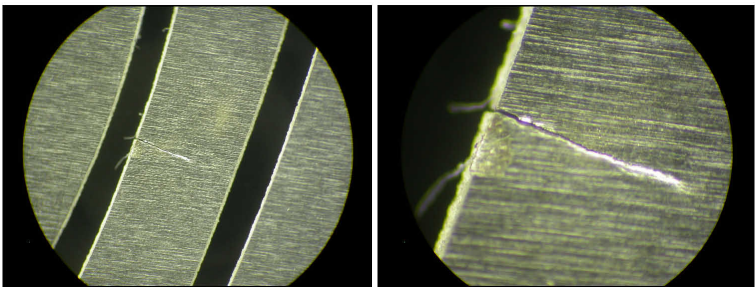

Figure 8. Spring 4 crack induced by fatigue. Note that the crack initiated at inner edge of Spring arm and propagated outwards.
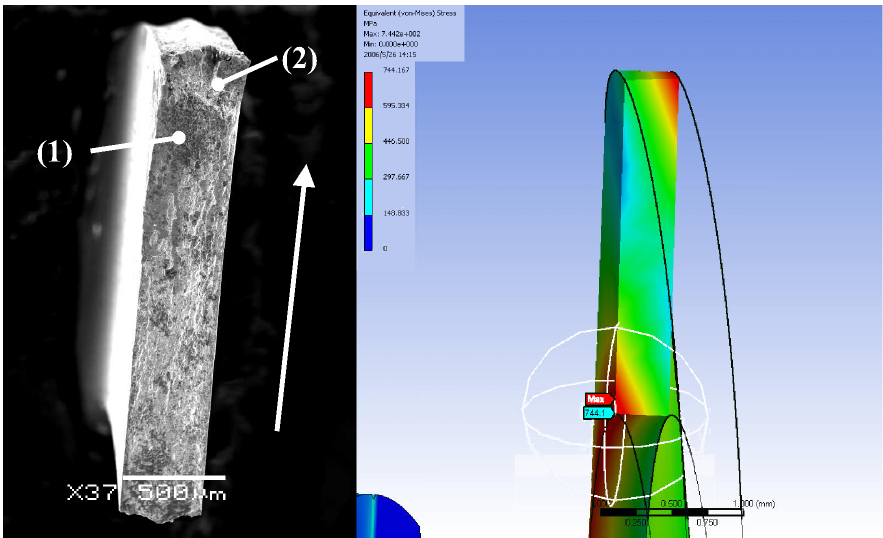

Figure 9. Spring 1 fatigue failure fracture face and FEA model section. Note the similarity of the stress patterns in the two images. The arrow indicates direction of crack growth, (1) indicates fast fracture, (2) indicates overload, i.e. final failure.

Theoretical Application

The spring which has been featured in the experimentation may be adopted as an example. Upon the assumption that the ultimate tensile strength (UTS) of the base material is 1275 MPa, and the endurance limit is 60% of the UTS, this indicates an endurance limit of 765 MPa. [Laboratory fatigue testing has been carried out by the author, on thin etched sheet tensile-type specimens, at an r ratio of 0.1. 10^6 cycle data has identified an endurance limit of ~700 MPa.] To avoid fatigue failure, components are designed to operate a suitable margin below the endurance limit.

[Note: - Laboratory data must be factored to account for the differences between the application and the testing environments, and the known statistical variations of the material. Due to the probabilistic nature of fatigue, values discussed are for median life, i.e. a reliability of 50%. The adjustment of endurance limit, in accordance with the Marin method is the result of six fractional factors, including reliability.]

Experimentation has suggested that for this variant of a spring, at maximum test stroke, 11.56 mm, superior quality control and batch testing is valid. Alternatively, by reducing the maximum stroke to 8 mm, the maximum stress may be reduced to within two-thirds of the laboratory endurance level (estimated as a reasonable factor of safety). By removing the risk of fatigue failure, the batch test procedure may be waived. Tensile testing of each etched sheet would be necessary to establish that material properties are within required limits. Detailed component inspection for key characteristics would continue to be a requirement.

CONCLUSIONS

Research and experimentation has improved understanding of spring displacement stroke versus stress. Constant stress regions have been established. Maximum stress location (for the investigated Spring) and failure initiation have been identified. Good data correlation between the FEA model and component test results support the use of FEA modelling for design optimization of flexure bearing springs. Research suggests that the FEA model is within 100 MPa of the mechanical stress experienced by the component. By using FEA tools, springs may be designed safely within their performance envelope, removing the need for batch testing. Operating below a known endurance limit, at a statistically established margin, well-designed springs may be assembled into products with a high level of confidence without batch testing. Advanced Stirling cryocooler springs which are optimized for a maximum stroke will continue to require superior quality control and batch testing.

FUTURE RESEARCH

To gain additional evidence, this work could be repeated on other variants of springs. FEA models have already been solved using alternative material data. Models including larger stacks of springs (say 4 off) may also be investigated. Mesh refinement may enhance results and the FEA model geometry may be improved by including the edge 'cusp'. Additional validation data may be gained by carrying out micro-hardness tests on springs which have been subjected to displacement and high-cycle fatigue. Identification of regions which have exceeded the elastic limit will serve as a supplementary check on the model prediction. Virgin as-etched springs may be used for reference.

ACKNOWLEDGMENTS

REFERENCES

1. ter Brake, H.J.M. and Wiegerinck, G.F.M, "Low-Power Cryocooler Survey," *Cryogenics,* Vol. 42, Issue: 11 (November 2002), pp. 705-718.

2. Bailey, P.B., Dadd, M.W., Hill, N., Cheuk, C.F., Raab, J. and Tward, E., "High Performance Flight Cryocooler Compressor," *Cryocoolers 11*, Kluwer Academic/Plenum Publishers, New York (2001), pp. 163-167.

3. Dadd, M.W., Bailey, P.B., Davey, G., Davis, T. and Tomlinson, B.J., "The Linearity of Clearance Seal Suspension Systems," *Cryocoolers 12*, Kluwer Academic/Plenum Publishers, New York (2003), pp. 255-264.

4. Gaunekar, A.S., Goddenhenrich, T. and Heiden, C., "Finite Element Analysis and Testing of Flexure Bearing Elements," *Cryogenics,* Vol. 36, Issue: 5 (May 1996), pp. 359-364.